

Signed Graph Metric Learning via Gershgorin Disc Alignment

Cheng Yang, *Member, IEEE*, Gene Cheung, *Senior Member, IEEE*, Wei Hu, *Member, IEEE*

Abstract—Given a convex and differentiable objective $Q(\mathbf{M})$ for a real, symmetric matrix \mathbf{M} in the positive definite (PD) cone—used to compute Mahalanobis distances—we propose a fast general metric learning framework that is entirely projection-free. We first assume that \mathbf{M} resides in a restricted space \mathcal{S} of generalized graph Laplacian matrices (graph metric matrices) corresponding to balanced signed graphs. Unlike low-rank metric matrices common in the literature, \mathcal{S} includes the important diagonal-only matrices as a special case. The key theorem to circumvent full eigen-decomposition and enable fast metric matrix optimization is Gershgorin disc alignment (GDA): given graph metric matrix $\mathbf{M} \in \mathcal{S}$ and diagonal matrix \mathbf{S} where $S_{ii} = 1/v_i$ and \mathbf{v} is the first eigenvector of \mathbf{M} , we prove that Gershgorin disc left-ends of similar transform $\mathbf{B} = \mathbf{S}\mathbf{M}\mathbf{S}^{-1}$ are perfectly aligned at the smallest eigenvalue λ_{\min} . Using this theorem, we replace the PD cone constraint in the metric learning problem with tightest possible signal-adaptive linear constraints, so that the alternating optimization of the diagonal / off-diagonal terms in \mathbf{M} can be solved efficiently as linear programs via Frank-Wolfe iterations. We update \mathbf{v} using Locally Optimal Block Preconditioned Conjugate Gradient (LOBPCG) with warm start as matrix entries in \mathbf{M} are optimized successively. Experiments show that our graph metric optimization is significantly faster than cone-projection methods, and produces competitive binary classification performance.

Index Terms—Graph signal processing, metric learning, Gershgorin circle theorem, convex optimization

1 INTRODUCTION

The notion of *feature distance* δ_{ij} between two data samples i and j , equipped with respective feature vectors $\mathbf{f}_i, \mathbf{f}_j \in \mathbb{R}^K$, is important for many machine learning problems such as graph-based classification [1]. Feature distance is traditionally computed as the *Mahalanobis distance* [2] $\delta_{ij} = (\mathbf{f}_i - \mathbf{f}_j)^\top \mathbf{M} (\mathbf{f}_i - \mathbf{f}_j)$, where \mathbf{M} is a *metric matrix* assumed to be positive definite (PD) [3]. How to determine the best metric \mathbf{M} —minimizing a given objective function $Q(\mathbf{M})$ subject to $\mathbf{M} \succ 0$ —is the *metric learning* problem. We focus on this optimization $\min_{\mathbf{M} \succ 0} Q(\mathbf{M})$ in this paper.

There is extensive prior work on the metric learning topic [4], [5], [6], [7], [8], [9]. One common challenge

in metric learning is to satisfy the PD cone constraint $\mathbf{M} \succ 0$ when minimizing $Q(\mathbf{M})$ in an efficient manner. A standard approach is alternating gradient-descent / projection (e.g., *proximal gradient* (PG) [10]), where a descent step α from current solution \mathbf{M}^t at iteration t in the direction of negative gradient $-\nabla Q(\mathbf{M}^t)$ is followed by a projection $\text{Proj}()$ back to the PD cone, i.e., $\mathbf{M}^{t+1} := \text{Proj}(\mathbf{M}^t - \alpha \nabla Q(\mathbf{M}^t))$. However, projection $\text{Proj}()$ typically requires eigen-decomposition of \mathbf{M} and soft-thresholding of its eigenvalues, which is expensive.

To avoid eigen-decomposition, recent methods consider alternative search spaces of matrices such as sparse or low-rank matrices to ease optimization [11], [12], [13], [4], [5]. While efficient, the assumed restricted search spaces often degrade the quality of sought metric \mathbf{M} in defining the Mahalanobis distance. For example, low-rank methods explicitly assume reducibility of the K available features to a lower dimension, and hence exclude the simple yet important weighted feature metric case where \mathbf{M} is diagonal [14], i.e., $(\mathbf{f}_i - \mathbf{f}_j)^\top \mathbf{M} (\mathbf{f}_i - \mathbf{f}_j) = \sum_k M_{k,k} (f_i^k - f_j^k)^2$, $m_{k,k} > 0, \forall k$.

In this paper, we propose a fast, general metric learning framework, capable of optimizing any convex differentiable objective $Q(\mathbf{M})$, that entirely circumvents eigen-decomposition-based projection on the PD cone. Compared to low-rank methods [13], [4], our framework is more inclusive and includes diagonal metric matrices as a special case. Specifically, we first define a search space \mathcal{S} of general graph Laplacian matrices [15], each corresponding to a balanced signed graph—we call these matrices *graph metric matrices*. In essence, an underlying graph \mathcal{G} corresponding to $\mathbf{M} \in \mathcal{S}$ contains: i) edge weights capturing pairwise (anti-)correlations among the K features, and ii) self-loops designating relative importance among the features.

The key to fast execution is a fundamental theorem called *Gershgorin disc alignment* (GDA) stating that for any metric $\mathbf{M} \in \mathcal{S}$, Gershgorin disc left-ends of similar transform $\mathbf{B} = \mathbf{S}\mathbf{M}\mathbf{S}^{-1}$, where \mathbf{S} is a diagonal matrix with $S_{ii} = 1/v_i$ and \mathbf{v} is the first eigenvector of \mathbf{M} , can be perfectly aligned at the smallest eigenvalue λ_{\min} . Leveraging this theorem, we next replace the PD cone constraint with a set of K signal-adaptive linear constraints as follows: i) compute scalars $S_{ii} = 1/v_i$ from

Cheng Yang and Gene Cheung are with York University, Toronto M3J 1P3, ON, Canada (e-mails: cheng.yang@ieee.org, gene@yorku.ca).

Wei Hu is with Peking University, Beijing 100871, China (e-mail: forihuwei@pku.edu.cn).

Gene Cheung acknowledges the support of the NSERC grants [RGPIN-2019-06271], [RGPAS-2019-00110].

Wei Hu acknowledges the support of National Natural Science Foundation of China (61972009) and Beijing Natural Science Foundation (4194080).

first eigenvector \mathbf{v} of previous solution \mathbf{M}^t , ii) write K linear constraints for K rows of the next solution \mathbf{M}^{t+1} using computed scalars S_{ii} to ensure PDness of \mathbf{M}^{t+1} via the Gershgorin Circle Theorem (GCT) [16]. Linear constraints mean that our proposed alternating optimization of the diagonal / off-diagonal terms in \mathbf{M}^{t+1} can be solved speedily as linear programs (LP) [17] via Frank-Wolfe iterations [18].

The bulk of the complexity resides in the repeated computation of the first eigenvectors \mathbf{v} of \mathbf{M}^t . We update \mathbf{v} iteratively using *Locally Optimal Block Preconditioned Conjugate Gradient* (LOBPCG) [19] with warm start as diagonal / off-diagonal terms are optimized progressively. Experiments show that our graph metric optimization is significantly faster than cone-projection methods, and produces competitive binary classification performance.

2 RELATED WORK

Existing metric learning methods can be divided into two main categories: linear distance metric learning and nonlinear distance metric learning.

2.1 Linear Distance Metric Learning

These methods learn linear transformations to project samples into a new feature space. This paradigm is prevalent in the metric learning community as many of the resulting transformations are tractable. Mahalanobis distance metric is one representative linear metric, which has been extensively studied under a variety of assumptions. Among them, some methods assume that the desired metric \mathbf{M} inherently lies in a lower dimension than the original K -dimensional feature space, and utilize projections such as Principle Component Analysis (PCA) [20] and random projection [21]. However, the employed projections can be computationally expensive, while yielding sub-optimal solutions due to reduced dimensionality. Some methods make structural assumptions on the sought metric matrix to ease optimization, such as low rank [13], [4] and sparsity [11], [12]. For example, Liu *et al.* propose convex and low-rank metric learning, which decomposes the learning task into two steps: an SVD-based projection and a metric learning problem with reduced dimensionality [13]. Other assumptions enforce the distance metric to be a diagonal matrix [22] or a sparse matrix [11], [12]. However, the structural assumptions of the metric matrix are often too strong, resulting in severely restricted search spaces and sub-optimal metrics.

2.2 Nonlinear Distance Metric Learning

Given possibly nonlinear relationship of data points, these methods learn nonlinear transformations to map samples into another feature space. While kernelized linear transformations can be adopted to address the nonlinearity problem [23], [24], [25], [26], choosing a kernel is typically difficult and empirical, and often not

flexible enough to capture the nonlinearity in the data. Motivated by the fact that deep learning is effective in modeling the nonlinearity of samples, deep metric learning (DML) methods have been proposed in recent years, which exploit the architecture of neural networks in deep learning to learn a set of hierarchical nonlinear transformations for nonlinear mapping of data points [27]. There are mainly two typical types of neural networks employed in DML methods: Siamese networks and triplet networks. DML methods based on Siamese networks include [28], [29], [30], [31], [32], [33], [34], while DML methods based on triplet networks include [35], [36], [37], [38], [39], [40], [41], [42]. Also, some DML methods employ other networks, such as [43], [44]. DML has shown substantial benefits in wide applications of various visual understanding tasks such as face recognition, image classification, visual search, person reidentification, visual tracking and so on. The objective functions are often designed for different specific tasks.

In this work, we focus on a class of objectives that are convex and differentiable, which can be linear or nonlinear. Many previous works target at such convex and differentiable objectives, including [45], [20], [46], [47].

2.3 GDA-based Graph Sampling

We have studied Gershgorin disc alignment (GDA) in the context of graph sampling in our previous work [48], [49], where the effect of choosing a graph node as sample is right-shifting a Gershgorin disc and scaling its neighboring nodes' discs in a breadth-first search (BFS) order. This results in an increase in the smallest Gershgorin disc left-end (lower bound of λ_{\min}), which in turn reduces the worst-case graph signal reconstruction error. There are two key difference between our current work and [48], [49]: i) we derive theorems to show *perfect* alignment of Gershgorin disc left-ends at λ_{\min} for defined classes of matrices, while alignment in [48], [49] is only approximate; and ii) we employ GDA in a formal optimization framework for metric learning.

Our recent work on GDA for metric learning [50] assumes a restricted search space of Laplacian matrices for irreducible *positive* graphs with positive degrees. Here we generalize to a much larger space of Laplacian matrices for *balanced signed* graphs. We will show in Section 6 that this generalization leads to noticeable performance gain when learning different metrics.

3 GERSHGORIN DISC ALIGNMENT

We first review basic definitions in graph signal processing (GSP) [51] that are necessary to understand our GDA theory. We then describe GDA for positive graphs and signed graphs in order.

3.1 Graph and Graph Laplacian Matrices

We consider an undirected graph $\mathcal{G} = \{\mathcal{N}, \mathcal{E}, \mathcal{U}\}$ containing a node set \mathcal{N} of cardinality $|\mathcal{N}| = K$. Each inter-node edge $(i, j) \in \mathcal{E}$, $i \neq j$, has an associated weight $w_{ij} \in \mathbb{R}$ that reflects the degree of (dis)similarity or (anti-)correlation between nodes i and j , depending on whether w_{ij} is positive or negative. Each node i may also have a self-loop $(i) \in \mathcal{U}$ with weight $u_i \in \mathbb{R}$.

One can collect edge weights and self-loops into an *adjacency matrix* \mathbf{W} , where $W_{ij} = w_{ij}$, $(i, j) \in \mathcal{E}$, and $W_{ii} = u_i$, $(i) \in \mathcal{U}$. We define $\mathbf{D} = \mathbf{W}1$ as a diagonal *degree matrix* that accounts for both inter-node edges and self-loops (1 is a column vector of all one's). The *combinatorial graph Laplacian matrix* [52] is defined as $\mathbf{L} = \mathbf{D} - \mathbf{W}$. A *generalized graph Laplacian matrix* [15] accounts for self-loops in \mathcal{G} also and is defined as $\mathbf{L}_g = \mathbf{D} - \mathbf{W} + \text{diag}(\mathbf{W})$, where $\text{diag}(\mathbf{W})$ extracts the diagonal entries of \mathbf{W} . Alternatively, we can write $\mathbf{L}_g = \mathbf{D} - \mathbf{W}_g$, where $\mathbf{W}_g = \mathbf{W} - \text{diag}(\mathbf{W})$ contains only inter-node edge weights (diagonal terms are zeros).

3.2 GDA for Positive Graphs

Consider first the simpler case of a *positive graph*, where an irreducible¹ graph \mathcal{G} (no disconnected nodes) has strictly positive edge weights and self-loops, *i.e.*, $w_{ij} > 0$, $(i, j) \in \mathcal{E}$ and $u_i > 0$, $(i) \in \mathcal{U}$. This means that \mathbf{W} is non-negative, the diagonals in \mathbf{D} are strictly positive, and the generalized graph Laplacian \mathbf{L}_g is positive semi-definite (PSD) [54]. We discuss first GDA for this case.

3.2.1 Gershgorin Circle Theorem

We first overview *Gershgorin Circle Theorem* (GCT) [16]. By GCT, each real eigenvalue λ of a real symmetric matrix \mathbf{M} resides in at least one *Gershgorin disc* Ψ_i , corresponding to row i of \mathbf{M} , with center $c_i = M_{ii}$ and radius $r_i = \sum_{j \mid j \neq i} |M_{ij}|$, *i.e.*,

$$\exists i \text{ s.t. } c_i - r_i \leq \lambda \leq c_i + r_i \quad (1)$$

Thus a sufficient (but not necessary) condition to guarantee that \mathbf{M} is PSD (smallest eigenvalue $\lambda_{\min} \geq 0$) is to ensure that the smallest Gershgorin disc left-end λ_{\min}^- —a lower bound for λ_{\min} —is non-negative, *i.e.*,

$$0 \leq \lambda_{\min}^- = \min_i c_i - r_i \leq \lambda_{\min} \quad (2)$$

However, λ_{\min}^- is often much smaller λ_{\min} , resulting in a loose lower bound. As an illustration, consider the following example 3×3 PSD matrix \mathbf{M} :

$$\mathbf{M} = \begin{bmatrix} 2 & -2 & -1 \\ -2 & 5 & -2 \\ -1 & -2 & 4 \end{bmatrix} \quad (3)$$

Lower bound $\lambda_{\min}^- = \min(-1, 1, 1) = -1$, while the smallest eigenvalue for \mathbf{M} is $\lambda_{\min} = 0.1078 > 0$. See Fig. 1 for an illustration of Gershgorin discs for this example.

1. An irreducible graph \mathcal{G} means that there exists a path from any node in \mathcal{G} to any other node in \mathcal{G} [53].

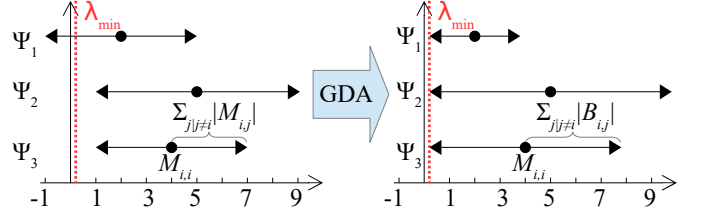


Fig. 1. Illustration of Gershgorin discs for matrix \mathbf{M} in (3) (left), and aligned discs for $\mathbf{B} = \mathbf{S}\mathbf{M}\mathbf{S}^{-1}$ (right).

3.2.2 GDA Analysis for Positive Graphs

GDA is a procedure to scale the Gershgorin disc radii r_i of matrix \mathbf{M} , so that their left-ends $c_i - r_i$ are perfectly aligned at the same value, precisely when $\lambda_{\min}^- = \lambda_{\min}$. Specifically, we perform a *similarity transform* [55] of \mathbf{M} via matrix \mathbf{S} , *i.e.*,

$$\mathbf{B} = \mathbf{S}\mathbf{M}\mathbf{S}^{-1} \quad (4)$$

where $\mathbf{S} = \text{diag}(s_1, \dots, s_K)$ is chosen to be a diagonal *scaling matrix* with scalars s_1, \dots, s_K along its diagonal, where $s_i > 0$, $\forall i$. \mathbf{B} has the same eigenvalues as \mathbf{M} , and thus the smallest Gershgorin disc left-end for \mathbf{B} is also a lower bound for \mathbf{M} 's smallest eigenvalue λ_{\min} , *i.e.*,

$$\lambda_{\min}^-(\mathbf{B}) \leq \lambda_{\min}(\mathbf{B}) = \lambda_{\min}(\mathbf{M}) \quad (5)$$

$$= \min_i B_{ii} - \sum_{j \mid j \neq i} |B_{ij}| \quad (6)$$

$$= \min_i M_{ii} - s_i \sum_{j \mid j \neq i} |M_{ij}|/s_j \quad (7)$$

We show that given a generalized graph Laplacian matrix \mathbf{M} corresponding to an irreducible, positive graph \mathcal{G} , there exist scalars s_1, \dots, s_K such that all Gershgorin disc left-ends are aligned at exactly λ_{\min} . We state this formally as a theorem.

Theorem 1. *Let \mathbf{M} be a generalized graph Laplacian matrix corresponding to an irreducible, positive graph \mathcal{G} . Denote by \mathbf{v} the first eigenvector of \mathbf{M} corresponding to the smallest eigenvalue λ_{\min} . Then by compute scalars $s_i = 1/v_i$, $\forall i$, all Gershgorin disc left-ends of $\mathbf{B} = \mathbf{S}\mathbf{M}\mathbf{S}^{-1}$, $\mathbf{S} = \text{diag}(s_1, \dots, s_K)$, are aligned at λ_{\min} , *i.e.*, $B_{ii} - \sum_{j \mid j \neq i} |B_{ij}| = \lambda_{\min}$, $\forall i$.*

Continuing our earlier example, using $s_1 = 0.7511$, $s_2 = 0.4886$ and $s_3 = 0.4440$, we see that $\mathbf{B} = \mathbf{S}\mathbf{M}\mathbf{S}^{-1}$ for \mathbf{M} in (3) has all disc left-ends aligned at $\lambda_{\min} = 0.1078$.

To prove Theorem 1, we first establish the following lemma.

Lemma 1. *There exists a first eigenvector \mathbf{v} with strictly positive entries for a generalized graph Laplacian matrix \mathbf{M} corresponding to an irreducible, positive graph \mathcal{G} .*

Proof: By definition, \mathbf{M} is a generalized graph Laplacian $\mathbf{M} = \mathbf{D} - \mathbf{W}_g$ with positive inter-node edge weights in \mathbf{W}_g and positive degrees in \mathbf{D} . Let \mathbf{v} be the first

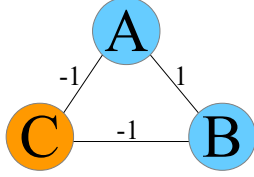


Fig. 2. Examples of a 3-node balanced signed graph (left) and an unbalanced signed graph (right).

eigenvector of \mathbf{M} , *i.e.*,

$$\begin{aligned}\mathbf{M}\mathbf{v} &= \lambda_{\min}\mathbf{v} \\ (\mathbf{D} - \mathbf{W}_g)\mathbf{v} &= (\lambda_{\min}\mathbf{I})\mathbf{v} \\ \mathbf{D}\mathbf{v} &= (\mathbf{W}_g + \lambda_{\min}\mathbf{I})\mathbf{v} \\ \mathbf{v} &= \mathbf{D}^{-1}(\mathbf{W}_g + \lambda_{\min}\mathbf{I})\mathbf{v}\end{aligned}$$

where $\lambda_{\min} \geq 0$ since \mathbf{M} is PSD. Since the matrix on the right contains only non-negative entries and \mathbf{W}_g is an irreducible matrix (graph \mathcal{G} is irreducible), \mathbf{v} is a positive eigenvector by the Perron-Frobenius Theorem [56]. \square

We now prove Theorem 1 as follows.

Proof: Denote by \mathbf{v} a strictly positive eigenvector corresponding to the smallest eigenvalue λ_{\min} of \mathbf{M} . Define $\mathbf{S} = \text{diag}(1/v_1, \dots, 1/v_K)$. Then,

$$\mathbf{S}\mathbf{M}\mathbf{S}^{-1}\mathbf{S}\mathbf{v} = \lambda_{\min}\mathbf{S}\mathbf{v} \quad (8)$$

where $\mathbf{S}\mathbf{v} = \mathbf{1} = [1, \dots, 1]^\top$. Let $\mathbf{B} = \mathbf{S}\mathbf{M}\mathbf{S}^{-1}$. Then,

$$\mathbf{B}\mathbf{1} = \lambda_{\min}\mathbf{1} \quad (9)$$

(9) means that

$$B_{ii} + \sum_{j \mid j \neq i} B_{ij} = \lambda_{\min}, \quad \forall i$$

Note that the off-diagonal terms $B_{ij} = (v_i/v_j)M_{ij} \leq 0$, since: i) \mathbf{v} is strictly positive, and ii) off-diagonal terms of generalized graph Laplacian \mathbf{M} for a positive graph satisfy $M_{i,j} \leq 0$. Thus,

$$B_{ii} - \sum_{j \mid j \neq i} |B_{ij}| = \lambda_{\min}, \quad \forall i \quad (10)$$

Thus, defining $\mathbf{S} = \text{diag}(1/v_1, \dots, 1/v_K)$ means $\mathbf{B} = \mathbf{S}\mathbf{M}\mathbf{S}^{-1}$ has all its Gershgorin disc left-ends aligned at λ_{\min} . \square

3.3 GDA for Signed Graphs

We generalize our GDA analysis to signed graphs, where weights for edges and self-loops can be negative. Central to our analysis is the concept of *graph balance*. We first discuss graph balance and the related Cartwright-Harary Theorem (CHT) [57], then present our GDA analysis.

3.3.1 Cartwright-Harary Theorem

The concept of balance in a signed graph has been studied in many scientific disciplines, including psychology,

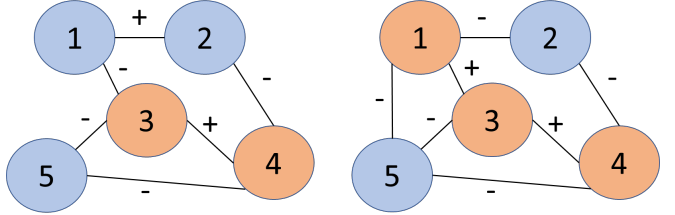


Fig. 3. Example of two 5-node balanced graphs. Node 1 has turned from blue to red from the left to the right.

social networks and data mining [58]. We employ the following common definition of a balance graph for our analysis:

Definition 1. A signed graph \mathcal{G} is balanced if \mathcal{G} does not contain any cycle with odd number of negative edges.

For intuition, consider a simple graph \mathcal{G} with three nodes denoted by A , B and C . Suppose that a positive/negative edge reflects pairwise friend/enemy relationship. An edge assignment of $(A, B) = 1$ and $(B, C) = (C, A) = -1$ —resulting in a cycle of two negative edges—means that A and B are friends, and that both A and B are enemies with C . See Fig. 2 for an illustration. This graph is balanced; entities in the graph can be grouped into two clusters, $\{A, B\}$ and $\{C\}$, where entities within a cluster are friends and entities across clusters are enemies.

On the other hand, an edge assignment of $(A, B) = (B, C) = 1$ and $(C, A) = -1$ —resulting in a cycle of one negative edge—means that both A and C are friends with B , but A and C are enemies. This graph is not balanced; one cannot assign entities to two distinct clusters with consistent signs as we did previously. We can generalize this example to the CHT [57], which we rephrase in abstract graph terminology as follows.

Theorem 2. A graph \mathcal{G} is balanced if its nodes \mathcal{N} can be partitioned into blue and red clusters, \mathcal{N}_b and \mathcal{N}_r , such that a positive edge always connects two nodes of the same color, and a negative edge always connects two nodes of the opposite colors.

See [57] for a formal proof. There are two important implications of CHT. First, to determine if \mathcal{G} is balanced, instead of examining all possible cycles in a graph \mathcal{G} and checking if each contains an odd number of negative edges, one can design a linear-time algorithm based on two-coloring. Second, we can use CHT to prove that GDA is possible for an irreducible, balanced signed graph. We describe this next.

3.3.2 GDA Analysis for Signed Graphs

Consider an irreducible, balanced signed graph $\mathcal{G}(\mathcal{N}, \mathcal{E}^+ \cup \mathcal{E}^-, \mathcal{U})$ with nodes \mathcal{N} , positive and negative inter-node edges, \mathcal{E}^+ and \mathcal{E}^- , and self-loops \mathcal{U} . According to CHT, nodes \mathcal{N} can be partitioned into blue and red clusters, \mathcal{N}_b and \mathcal{N}_r , such that

- 1) $(i, j) \in \mathcal{E}^+$ implies that either $i, j \in \mathcal{N}_b$ or $i, j \in \mathcal{N}_r$.
- 2) $(i, j) \in \mathcal{E}^-$ implies that either $i \in \mathcal{N}_b$ and $j \in \mathcal{N}_r$, or $i \in \mathcal{N}_r$ and $j \in \mathcal{N}_b$.

As an example, consider the 5-node balanced graph in Fig. 3, where nodes 1, 2 and 5 are colored blue, while nodes 3 and 4 are colored red. Only positive edges connect nodes of the same colors, while negative edges connect nodes of the opposite colors. There does not exist a cycle of odd number of negative edges in this graph.

We now state a generalization of Theorem 1 to balanced signed graphs as follows:

Theorem 3. Denote by \mathbf{M} a generalized graph Laplacian matrix corresponding to an irreducible, balanced signed graph \mathcal{G} . Denote by \mathbf{v} the first eigenvector of \mathbf{M} corresponding to the smallest eigenvalue λ_{\min} . Define $\mathbf{B} = \mathbf{S}\mathbf{M}\mathbf{S}^{-1}$ as a similarity transform of \mathbf{M} , where $\mathbf{S} = \text{diag}(s_1, \dots, s_N)$. If $s_i = 1/v_i$, where $v_i \neq 0, \forall i$, then Gershgorin disc left-ends of \mathbf{B} are aligned at λ_{\min} , i.e., $B_{ii} - \sum_{j|j \neq i} |B_{ij}| = \lambda_{\min}, \forall i$.

We prove this theorem as follows.

Proof: We first reorder blue nodes before red nodes in the rows and columns of \mathbf{M} , so that \mathbf{M} can be written as a 2×2 block matrix as follows:

$$\mathbf{M} = \begin{bmatrix} \mathbf{M}_{11} & \mathbf{M}_{12} \\ \mathbf{M}_{12}^\top & \mathbf{M}_{22} \end{bmatrix} \quad (11)$$

where off-diagonal terms in \mathbf{M}_{11} (\mathbf{M}_{22}) are negative stemming from positive edge weights $w_{ij} \geq 0$ connecting same-color nodes, and entries in \mathbf{M}_{12} are positive stemming from negative edge weights $w_{ij} \leq 0$ connecting different-color nodes. Define now a similarity transform \mathbf{M}' of \mathbf{M} :

$$\mathbf{M}' = \begin{bmatrix} \mathbf{I}_b & \mathbf{0} \\ \mathbf{0} & -\mathbf{I}_r \end{bmatrix} \begin{bmatrix} \mathbf{M}_{11} & \mathbf{M}_{12} \\ \mathbf{M}_{12}^\top & \mathbf{M}_{22} \end{bmatrix} \begin{bmatrix} \mathbf{I}_b & \mathbf{0} \\ \mathbf{0} & -\mathbf{I}_r \end{bmatrix} \quad (12)$$

$$= \begin{bmatrix} \mathbf{M}_{11} & -\mathbf{M}_{12} \\ -\mathbf{M}_{12}^\top & \mathbf{M}_{22} \end{bmatrix} \quad (13)$$

$\mathbf{M}' = \mathbf{D} + \mathbf{W}_g'$ can be interpreted as a generalized graph Laplacian matrix for a new graph $\mathcal{G}'(\mathcal{N}, \mathcal{E}', \mathcal{U}')$ corresponding to \mathcal{G} , where \mathcal{G}' keeps all positive edges \mathcal{E}^+ , but for each negative edge \mathcal{E}^- , \mathcal{G}' switches its sign to positive. Thus,

$$w'_{ij} = \begin{cases} w_{ij} & \text{if } (i, j) \in \mathcal{E}^+ \\ -w_{ij} & \text{if } (i, j) \in \mathcal{E}^- \end{cases} \quad (14)$$

To maintain the same degree matrix \mathbf{D} as \mathcal{G} , each node i in \mathcal{G}' has a self-loop with weight u'_i defined as

$$u'_i = u_i + 2 \sum_{j|j \neq i} w_{ij} \quad (15)$$

As a similarity transform, \mathbf{M} and \mathbf{M}' have the same eigenvalues, and an eigenvector \mathbf{z} for \mathbf{M}' maps to an eigenvector \mathbf{v} for \mathbf{M} as follows:

$$\mathbf{v} = \begin{bmatrix} \mathbf{I}_b & \mathbf{0} \\ \mathbf{0} & -\mathbf{I}_r \end{bmatrix} \mathbf{z} \quad (16)$$

Finally, we define a shifted graph Laplacian matrix

$\mathbf{M}'' = \mathbf{M}' + \epsilon \mathbf{I}$, where constant $\epsilon > 0$ is

$$\epsilon > \max_i \left\{ - \sum_{j|(i,j) \in \mathcal{E}^+ \cup \mathcal{E}^-} w_{ij} - u_i \right\} \quad (17)$$

\mathbf{M}'' has the same set of eigenvectors as \mathbf{M}' , and its eigenvalues are the same as \mathbf{M}' but offset by ϵ .

\mathbf{M}'' has strictly positive node degrees D''_{ii} , i.e.,

$$\begin{aligned} D''_{ii} &= \sum_{j|(i,j) \in \mathcal{E}'} w'_{ij} + u'_i + \epsilon \\ &= \sum_{j|(i,j) \in \mathcal{E}^+} w_{ij} - \sum_{j|(i,j) \in \mathcal{E}^-} w_{ij} + u_i + 2 \sum_{j|(i,j) \in \mathcal{E}^-} w_{ij} + \epsilon \\ &= \sum_{j|(i,j) \in \mathcal{E}^+} w_{ij} + \sum_{j|(i,j) \in \mathcal{E}^-} w_{ij} + u_i + \epsilon \stackrel{(a)}{>} 0 \end{aligned}$$

The inequality in (a) is due to the assumed inequality for ϵ in (17).

From Theorem 1, given \mathbf{M}'' is a generalized graph Laplacian matrix for an irreducible graph with positive edges and degrees, first eigenvector of \mathbf{M}'' (also first eigenvector of \mathbf{M}') \mathbf{z} is a strictly positive vector. Thus, corresponding \mathbf{v} for \mathbf{M} is a strictly non-zero first eigenvector, i.e., $v_i \neq 0, \forall i$.

Having established first eigenvector \mathbf{v} of \mathbf{M} , we can define diagonal matrix $\mathbf{S} = \text{diag}(1/v_1, \dots, 1/v_N)$, and write

$$\mathbf{S}\mathbf{M}\mathbf{S}^{-1}\mathbf{v} = \lambda_{\min}\mathbf{S}\mathbf{v} \quad (18)$$

$$\mathbf{B}\mathbf{1} = \lambda_{\min}\mathbf{1} \quad (19)$$

where $\mathbf{B} = \mathbf{S}\mathbf{M}\mathbf{S}^{-1}$. Each row i in (19) states that

$$B_{ii} + \sum_{j|j \neq i} B_{ij} = \lambda_{\min} \quad (20)$$

$$M_{ii} + s_i \sum_{j|j \neq i} M_{ij}/s_j = \lambda_{\min} \quad (21)$$

Suppose i is a red node. Then $v_i = -z_i < 0$, and thus $s_i = 1/v_i < 0$. For each red neighbor j of i , $s_j < 0$, and $w_{ij} > 0$ means that $M_{ij} < 0$. We can hence conclude that $s_i M_{ij}/s_j < 0$ and $s_i M_{ij}/s_j = -|s_i M_{ij}/s_j|$. For each blue neighbor j of i , $s_j > 0$, and $w_{ij} < 0$ means that $M_{ij} > 0$. We can hence conclude also that $s_i M_{ij}/s_j < 0$ and $s_i M_{ij}/s_j = -|s_i M_{ij}/s_j|$. Similar analysis can be performed if i is a blue node. Thus (21) can be rewritten as

$$M_{ii} - \sum_{j|j \neq i} |s_i M_{ij}/s_j| = \lambda_{\min} \quad (22)$$

In other words, left-end of \mathbf{B} 's i -th Gershgorin disc—centre M_{ii} minus radius $\sum_{j \neq i} |s_i M_{ij}/s_j|$ —is aligned at λ_{\min} . This holds true for all i . \square

4 OPTIMIZING METRIC DIAGONALS

We now use GDA to optimize a metric matrix \mathbf{M} . We first define our search space of metric matrices and our problem to optimize \mathbf{M} 's diagonal terms. We then

describe how GDA can be used in combination with the Frank-Wolfe method to speed up our optimization.

4.1 Search Space of Graph Metric Matrices

We assume that associated with each data sample i is a length- K feature vector $\mathbf{f}_i \in \mathbb{R}^K$. A *metric matrix* $\mathbf{M} \in \mathbb{R}^{K \times K}$ defines the feature distance $\delta_{ij}(\mathbf{M})$ —the *Mahalanobis distance* [2]—between samples i and j as:

$$\delta_{ij}(\mathbf{M}) = (\mathbf{f}_i - \mathbf{f}_j)^\top \mathbf{M} (\mathbf{f}_i - \mathbf{f}_j) \quad (23)$$

By definition of a metric [3], one requires \mathbf{M} to be a *positive definite* (PD) matrix, denoted by $\mathbf{M} \succ 0$. This means that feature distance $\delta_{ij}(\mathbf{M})$ is strictly positive unless $\mathbf{f}_i = \mathbf{f}_j$, *i.e.*, $(\mathbf{f}_i - \mathbf{f}_j)^\top \mathbf{M} (\mathbf{f}_i - \mathbf{f}_j) > 0$ if $\mathbf{f}_i - \mathbf{f}_j \neq 0$.

To efficiently enforce $\mathbf{M} \succ 0$, we invoke our developed GDA theory that involves generalized graph Laplacian matrices. We define the search space \mathcal{S} of metric matrices for our optimization framework as follows:

Definition 2. \mathcal{S} is a space of real, symmetric matrices that are generalized graph Laplacian matrices corresponding to irreducible, balanced undirected signed graphs.

We call a matrix $\mathbf{M} \in \mathcal{S}$ that is also PD, denoted by $\mathbf{M} \succ 0$, a *graph metric matrix*.

4.2 Problem Formulation

We pose an optimization problem for \mathbf{M} : find an optimal graph metric \mathbf{M} —leading to feature distances $\delta_{ij}(\mathbf{M})$ in (23)—that yields the smallest value of a convex differential objective $Q(\{\delta_{ij}(\mathbf{M})\})$:

$$\min_{\mathbf{M} \in \mathcal{S}} Q(\{\delta_{ij}(\mathbf{M})\}), \quad \text{s.t. } \begin{cases} \text{tr}(\mathbf{M}) \leq C \\ \mathbf{M} \succ 0 \end{cases} \quad (24)$$

where $C > 0$ is a chosen parameter. Constraint $\text{tr}(\mathbf{M}) \leq C$ is needed to avoid pathological solutions with infinite feature distances, *i.e.*, $\delta_{ij}(\mathbf{M}) = \infty$. For stability, we assume also that the objective is lower-bounded, *i.e.*, $\min_{\mathbf{M} \succ 0} Q(\{\delta_{ij}(\mathbf{M})\}) \geq \kappa > -\infty$ for some constant κ . We discuss concrete examples of objective $Q(\{\delta_{ij}(\mathbf{M})\})$ in Section 6.

Our strategy to solve (24) is to optimize \mathbf{M} 's diagonal terms *plus* one row/column of off-diagonal terms at a time using the Frank-Wolfe (FW) iterative method [18], where each FW iteration is solved as an LP until convergence. We discuss first the initialization of \mathbf{M} , then the optimization setup for \mathbf{M} 's diagonal terms. For notation convenience, we will write the objective simply as $Q(\mathbf{M})$, with the understanding that metric \mathbf{M} computes first the feature distances $\delta_{ij}(\mathbf{M})$, which in turn determines the objective $Q(\{\delta_{ij}(\mathbf{M})\})$.

4.2.1 Initialization of Metric \mathbf{M}

We first initialize a valid graph metric \mathbf{M}^0 as follows:

- 1) Initialize each diagonal term $M_{ii}^0 := C/K$.
- 2) Initialize off-diagonal terms $M_{ij}^0, i \neq j$, as:

$$M_{ij}^0 := \begin{cases} \epsilon (-1)^{\min(i,j)} & \text{if } j = i \pm 1 \\ 0 & \text{o.w.} \end{cases} \quad (25)$$

where $\epsilon > 0$ is a small parameter. Initialization of the diagonal terms ensures that constraint $\text{tr}(\mathbf{M}^0) \leq C$ is satisfied. Initialization of the off-diagonal terms ensures that \mathbf{M}^0 is symmetric and PD ($C/K - |\epsilon| > 0$), and that the underlying graph \mathcal{G} is a chain with nodes connected by edges of alternating signs. Because \mathcal{G} is a chain graph, it is balanced. We can hence conclude that initial \mathbf{M}^0 is a graph metric, *i.e.*, $\mathbf{M}^0 \in \mathcal{S}$ and $\mathbf{M}^0 \succ 0$.

4.2.2 Optimization of Diagonals

Optimizing \mathbf{M} 's diagonal terms M_{ii} alone, (24) becomes

$$\begin{aligned} \min_{\{M_{ii}\}} \quad & Q(\mathbf{M}) \\ \text{s.t.} \quad & \mathbf{M} \succ 0; \quad \sum_i M_{ii} \leq C; \quad M_{ii} > 0, \forall i \end{aligned} \quad (26)$$

where $\text{tr}(\mathbf{M}) = \sum_i M_{ii}$. Because the diagonal terms do not affect the irreducibility and balance of matrix \mathbf{M} , the only requirement for \mathbf{M} to be a graph metric is just to ensure \mathbf{M} is PD.

4.3 Replacing PD Cone with GDA Linear Constraints

To efficiently enforce the PD constraint $\mathbf{M} \succ 0$, we derive sufficient (but not necessary) linear constraints using GCT [16]. A straightforward application of GCT directly on \mathbf{M} will translate to a linear constraint for each row i :

$$M_{ii} \geq \sum_{j \mid j \neq i} |M_{ij}| + \rho, \quad \forall i \in \{1, \dots, K\} \quad (27)$$

where $\rho > 0$ is a small parameter.

However, as discussed in Section 3.2.1, GCT lower bound $\lambda_{\min}^- = \min_i M_{ii} - \sum_{j \neq i} |M_{ij}|$ for λ_{\min} can be loose. When optimizing \mathbf{M} , enforcing (27) directly can mean a much more restricted space than the original $\{\mathbf{M} \mid \mathbf{M} \succ 0\}$ in (26), resulting in an inferior solution.

To derive more appropriate linear constraints—thus more suitable search spaces when solving $\min Q(\mathbf{M})$ —we leverage our GDA theory and examine instead the Gershgorin discs of a similarity-transformed matrix \mathbf{B} from \mathbf{M} , *i.e.*, $\mathbf{B} = \mathbf{S} \mathbf{M} \mathbf{S}^{-1}$, where $\mathbf{S} = \text{diag}(s_1, \dots, s_K)$. This leads to the following linear constraints instead:

$$M_{ii} \geq \sum_{j \mid j \neq i} \left| \frac{s_i M_{ij}}{s_j} \right| + \rho, \quad \forall i \in \{1, \dots, K\} \quad (28)$$

The crux is in the selection of scalars s_i . Suppose that the optimal solution to (26) is \mathbf{M}^* . Then, using the first eigenvector \mathbf{v}^* of \mathbf{M}^* corresponding to smallest eigenvalue $\lambda_{\min}^* > 0$, one can compute $s_i = 1/v_i^*$ to align all disc left-ends of $\mathbf{B} = \mathbf{S} \mathbf{M} \mathbf{S}^{-1}$ at λ_{\min}^* , so that optimal solution \mathbf{M}^* is in the search space defined by (28).

Of course, in practice we do not have solution \mathbf{M}^* available *a priori* to compute \mathbf{v}^* . Thus, we solve the optimization iteratively, where we use the previous solution \mathbf{M}^{t-1} at iteration $t-1$ to compute scalars s_i^t 's, solve for a better solution \mathbf{M}^t using linear constraints (28), compute new scalars again etc until convergence. Specifically,

1) Given scalars s_i^t 's, identify a good solution \mathbf{M}^t minimizing objective $Q(\mathbf{M})$ subject to (28), *i.e.*,

$$\min_{\{M_{ii}\}} Q(\mathbf{M}) \quad (29)$$

$$\text{s.t. } M_{ii} \geq \sum_{j \mid j \neq i} \left| \frac{s_i^t M_{ij}}{s_j^t} \right| + \rho, \forall i; \quad \sum_i M_{ii} \leq C$$

2) Given \mathbf{M}^t , update scalars $s_i^{t+1} = 1/v_i^t$ where \mathbf{v}^t is the first eigenvector of \mathbf{M}^t .

3) Increment t and repeat until convergence.

When the scalars in (29) are updated as $s_i^{t+1} = 1/v_i^t$ for iteration $t+1$, we show that previous solution \mathbf{M}^t at iteration t remains feasible at iteration $t+1$:

Lemma 2. *Solution \mathbf{M}^t to (29) in iteration t remains feasible in iteration $t+1$, when scalars s_i^{t+1} for the linear constraints in (29) are updated as $s_i^{t+1} = 1/v_i^t, \forall i$, where \mathbf{v}^t is the first eigenvector of \mathbf{M}^t .*

Proof: Using the first eigenvector \mathbf{v}^t of graph metric \mathbf{M}^t at iteration t , by the proof of Theorem 1 we know that the Gershgorin disc left-ends of $\mathbf{B} = \mathbf{S}\mathbf{M}^t\mathbf{S}^{-1}$ are aligned at λ_{\min} . Since \mathbf{M}^t is a feasible solution in (29), $\mathbf{M}^t \succ 0$ and $\lambda_{\min} > 0$. Thus \mathbf{M}^t is also a feasible solution when scalars are updated as $s_i = 1/v_i^t, \forall i$. \square

Given that the iterations continue to find better feasible solutions \mathbf{M} with smaller objectives $Q(\mathbf{M})$ and that $Q(\mathbf{M})$ is lower-bounded by κ by assumption, we can conclude that the loop converges to a local optimal solution where $\mathbf{M}^{t+1} = \mathbf{M}^t$.

The remaining issue is how to best compute first eigenvector \mathbf{v}^t given solution \mathbf{M}^t repeatedly. For this task, we employ *Locally Optimal Block Preconditioned Conjugate Gradient* (LOBPCG) [19], a fast algorithm known to compute extreme eigenpairs efficiently. Because LOBPCG is iterative, it benefits from *warm start*: algorithm converges much faster if a good solution initiates the iterations. In our case, we use previously computed eigenvector \mathbf{v}^{t-1} as an initial solution to speed up LOBPCG when computing \mathbf{v}^t , reducing its complexity substantially.

4.4 Frank-Wolfe Method

To solve (29), we employ the Frank-Wolfe (FW) method [18] that iteratively linearizes the objective $Q(\mathbf{M})$ using its gradient $\nabla Q(\mathbf{M}^t)$ with respect to diagonal terms $\{M_{ii}\}$, computed using previous solution \mathbf{M}^t , *i.e.*,

$$\nabla Q(\mathbf{M}^t) = \left[\begin{array}{c} \frac{\partial Q(\mathbf{M})}{\partial M_{1,1}} \\ \vdots \\ \frac{\partial Q(\mathbf{M})}{\partial M_{K,K}} \end{array} \right] \Big|_{\mathbf{M}^t} \quad (30)$$

Given gradient $\nabla Q(\mathbf{M}^t)$, optimization (29) becomes a *linear program* (LP) at each iteration t :

$$\begin{aligned} \min_{\{M_{ii}\}} & \text{vec}(\{M_{ii}\})^\top \nabla Q(\mathbf{M}^t) \\ \text{s.t. } & M_{ii} \geq \sum_{j \mid j \neq i} \left| \frac{s_i M_{ij}^t}{s_j} \right| + \rho, \quad \forall i; \quad \sum_i M_{ii} \leq C. \end{aligned} \quad (31)$$

where $\text{vec}(\{M_{ii}\}) = [M_{1,1} \ M_{2,2} \ \dots \ M_{K,K}]^\top$ is a vector composed of diagonal terms $\{M_{ii}\}$, and M_{ij}^t are off-diagonal terms of previous solution \mathbf{M}^t . LP (31) can be solved efficiently using known fast algorithms such as Simplex [17] and interior point method [59]. When a new solution $\{M_{ii}^{t+1}\}$ is obtained, gradient $\nabla Q(\mathbf{M}^{t+1})$ is updated, and LP (31) is solved again until convergence.

4.4.1 Step Size Optimization

Having found a solution $\{M_{ii}^*\}$ to LP (31), define *direction* $\{d_{ii}\}$ where $d_{ii} = M_{ii}^* - M_{ii}^k$. We now solve a one-dimensional optimization problem for step size γ :

$$\min_{\gamma \mid 0 \leq \gamma \leq 1} Q(\mathbf{M}^t + \gamma \text{diag}(\{d_{ii}\})) \quad (32)$$

where $\text{diag}(\{d_{ii}\})$ is a diagonal matrix with $\{d_{ii}\}$ along its diagonal entries. Define $\mathbf{M}^* = \mathbf{M}^t + \gamma \text{diag}(\{d_{ii}\})$. Using the chain rule for multivariate functions, we can write:

$$\frac{\partial Q(\mathbf{M}^*)}{\partial \gamma} = \sum_{i=1}^K \frac{\partial Q(\mathbf{M}^*)}{\partial M_{ii}^*} \frac{\partial M_{ii}^*}{\partial \gamma} \quad (33)$$

$$= \sum_{i=1}^K \frac{\partial Q(\mathbf{M}^*)}{\partial M_{ii}^*} d_{ii}. \quad (34)$$

Substituting $M_{ii}^* = M_{ii}^t + \gamma d_{ii}$ into (34), we can write $Q'(\gamma) = \frac{\partial Q(\mathbf{M}^*)}{\partial \gamma}$ as a function of γ only.

Since $Q(\mathbf{M})$ is convex, one-dimensional $Q(\gamma)$ is also convex, and $Q'(\gamma^*) = 0$ at a unique γ^* . In general, we cannot find γ^* in closed form given an arbitrary convex and differentiable $Q(\mathbf{M})$. However, one can approximate γ^* quickly given derived $Q'(\gamma)$ using any root-finding algorithms, such as the Newton-Raphson (NR) method [60]. Given the range restriction of γ in (32), our proposed procedure to find step size γ^t at iteration t is thus the following:

- 1) Derive $Q'(\gamma)$ using (34) and compute minimizing γ^* using NR.
- 2) Compute appropriate step size γ^t as follows:

$$\gamma^t = \begin{cases} 1 & \text{if } \gamma^* > 1 \\ 0 & \text{if } \gamma^* < 0 \\ \gamma^* & \text{o.w.} \end{cases} \quad (35)$$

The updated solution from FW iteration is then $\mathbf{M}^{t+1} = \mathbf{M}^t + \gamma^t \text{diag}(\{d_{ii}\})$.

4.4.2 Comparing Frank-Wolfe and Proximal Gradient

After rewriting the PD cone constraint to a series of signal-adaptive linear constraints—thus defining a (more restricted) convex feasible space \mathcal{S} that is a polytope, one can conceivably use proximal gradient (PG) [10] instead of FW to optimize $Q(\mathbf{M})$. PG alternately performs a gradient descent step followed by a proximal operator that is a projection back to \mathcal{S} until convergence [61]. First, FW is entirely project-free, while PG requires one convex set projection per iteration. More importantly, it is difficult in general to determine an optimal step

size for gradient descent in PG—one that makes the maximal progress without overshooting. In the literature [10], PG step size can be determined based on Lipschitz constant of $\nabla Q(\mathbf{M})$, which is expensive to compute if the Hessian matrix $\nabla^2 Q(\mathbf{M})$ is large. In contrast for FW, after direction $\{d_{ii}\}$ is determined in the first step, the objective $Q(\gamma)$ becomes one-dimensional, and thus optimal step size γ can be computed efficiently using first- and second-order information $Q'(\gamma)$ and $Q''(\gamma)$. In our experiments, we show indeed that our proposed FW-based optimization is more computation-efficient compared to a previous PG-based method [61].

5 OPTIMIZING METRIC OFF-DIAGONALS

Including off-diagonal terms of metric \mathbf{M} into the optimization is more complicated, since any modification of these terms may affect the balance and connectivity of the underlying graph. We design a block coordinate descent algorithm, which optimizes one row/column of off-diagonal terms plus diagonal terms at a time while maintaining graph balance.

5.1 Problem Formulation

First, we divide \mathbf{M} into four sub-matrices:

$$\mathbf{M} = \begin{bmatrix} \mathbf{M}_{1,1} & \mathbf{M}_{1,2} \\ \mathbf{M}_{2,1} & \mathbf{M}_{2,2} \end{bmatrix}, \quad (36)$$

where $\mathbf{M}_{1,1} \in \mathbb{R}$, $\mathbf{M}_{1,2} \in \mathbb{R}^{1 \times (K-1)}$, $\mathbf{M}_{2,1} \in \mathbb{R}^{(K-1) \times 1}$ and $\mathbf{M}_{2,2} \in \mathbb{R}^{(K-1) \times (K-1)}$. Assuming \mathbf{M} is symmetric, $\mathbf{M}_{1,2} = \mathbf{M}_{2,1}^\top$. We optimize $\mathbf{M}_{1,2}$ and $\{M_{ii}\}$ in one iteration, *i.e.*,

$$\min_{\mathbf{M}_{2,1}, \{M_{ii}\}} Q(\mathbf{M}), \quad \text{s.t.} \quad \begin{cases} \mathbf{M} \succ 0 \\ \mathbf{M} \in \mathcal{S} \\ \sum_i M_{ii} \leq C \end{cases} \quad (37)$$

In the next iteration, a different node is selected, and with appropriate row/column permutation, we still optimize the first column off-diagonals $\mathbf{M}_{2,1}$ as in (37). For \mathbf{M} to remain a graph metric, i) \mathbf{M} must be PD, ii) \mathbf{M} must be balanced, and iii) \mathbf{M} must be irreducible.

5.2 Maintaining Graph Balance

We maintain graph balance during off-diagonal optimization as follows. Assuming graph \mathcal{G} from previous solution \mathbf{M}^{t-1} is balanced, nodes \mathcal{N} are colored into blue nodes \mathcal{N}_b and red nodes \mathcal{N}_r . Suppose node 1 is a blue node. Then we constrain edge weights to other blue/red nodes to be positive/negative. Combining these sign constraints with previously discussed GDA-based linear constraints to replace the PD cone constraint, the optimi-

mization becomes:

$$\begin{aligned} \min_{\mathbf{M}_{2,1}, \{M_{ii}\}} \quad & Q(\mathbf{M}) \\ \text{s.t.} \quad & M_{i,i}^t \geq \sum_{j \mid j \neq i} \left| \frac{s_i^t M_{ij}}{s_j^t} \right| + \rho, \quad \forall i \\ & M_{i,1} \leq 0, \quad \text{if } i \in \mathcal{N}_b \\ & M_{i,1} \geq 0, \quad \text{if } i \in \mathcal{N}_r \\ & \sum_i M_{ii} \leq C \end{aligned} \quad (38)$$

Note that the sign for each $s_i^t M_{i,j} / s_j^t$ is known, given we know the scalar values s_i^t as well as the sign of $M_{i,j}$. Thus the absolute value operator can be appropriately removed, and the set of constraints remain linear.

Suppose instead node 1 is a red node. Then the last two edge sign constraints in (38) are replaced by

$$\begin{aligned} M_{i,1} \geq 0, \quad & \text{if } i \in \mathcal{N}_b \\ M_{i,1} \leq 0, \quad & \text{if } i \in \mathcal{N}_r \end{aligned}$$

After optimizing $\mathbf{M}_{2,1}$ twice, each time assuming node 1 is blue/red, we retain the better solution $\mathbf{M}_{2,1}^*$ that yields the smaller objective $Q(\mathbf{M})$. As an example, in Fig. 3 node 1's edges to other nodes are optimized assuming it is blue/red in the left/right graph. In both cases, the signs of the edge weights are constrained so that the graphs remain balanced.

(38) also has a convex differentiable objective with a set of linear constraints. We thus employ the FW method again to iteratively linearize the objective using gradient $\nabla Q(\mathbf{M}^t)$ with respect to off-diagonal $\mathbf{M}_{2,1}$, where the solution in each iteration is solved as an LP. We omit the details for brevity.

5.3 Disconnected Sub-Graphs

The previous optimization assumes that the underlying graph \mathcal{G} corresponding to the generalized graph Laplacian \mathbf{M} is irreducible. When optimizing off-diagonal terms in \mathbf{M} also, \mathcal{G} may become disconnected into P separate sub-graphs $\mathcal{G}_1, \dots, \mathcal{G}_P$, with corresponding generalized graph Laplacian matrices $\mathbf{M}_1, \dots, \mathbf{M}_P$, where $\mathbf{M} = \text{diag}(\mathbf{M}_1, \dots, \mathbf{M}_P)$, *i.e.*, \mathbf{M} is block-diagonal. In this case, to compute scalars s_i in (29), we simply compute the first eigenvector \mathbf{v}_p via LOBPCG for each matrix \mathbf{M}_p to derive scalars s_i for diagonals M_{ii} in \mathbf{M}_p . Optimization (29) can then be solved using the same FW method as described previously.

Given data $\mathbf{X} = [\mathbf{f}_1, \dots, \mathbf{f}_N]$, color set \mathbf{c}^0 and subgraph set \mathbf{g}^0 , we summarize our optimization framework called *signed graph metric learning* (SGML) in Algorithm 1.

6 EXPERIMENTS

We evaluate our signed graph metric learning (SGML) method in terms of 1) converged objective value (or final objective value after maximal number of iterations) of different convex and differentiable $Q(\mathbf{M})$'s against

Algorithm 1 Signed Graph Metric Learning (SGML).

Input: $\mathbf{X}, C = K, \mathbf{M}^0 \succ 0, \mathbf{c}^0, \mathbf{g}^0, \rho = 1e - 5$.
Output: \mathbf{M}^* .

```

1: compute scalars  $\{s_i^t\}$  via LOBPCG.
2: for  $i = 1 : K$ 
3:   while not converged do
4:     Solving (31) (dia-offdia version).
5:     while not converged do
6:       Solving (32).
7:     end while
8:   end while
9: check sub-graph  $\mathbf{g}_i$ , compute  $\{s_i^t\}$  via LOBPCG.
10: do 3-9 with  $c_i = 1$  and  $-1$ , respectively, and choose
    the solution whichever yields a better objective.
11: end for
12: while not converged do
13:   Solving (31) (full version).
14:   while not converged do
15:     Solving (32).
16:   end while
17: end while
18: return  $\mathbf{M}^*$ .

```

competing optimization schemes, 2) running time, and 3) performance in a specific application, namely binary classification, against competing metric learning schemes.

6.1 Converged objective value and running time

We compare converged objective values against the following two competing optimization schemes: 1) gradient descent with projection onto a positive-definite convex cone (PD-cone) for full \mathbf{M} optimization, and 2) gradient descent with projection onto the intersection of a half space and a box for diagonal entries and projection onto a norm ball (HBNB) for each row/column of off-diagonal entries [61].

We evaluate PD-cone, HBNB, and SGML on $Q(\mathbf{M})$'s that 1) are convex and (partially) differentiable, and 2) require \mathbf{M} to be PD. Specifically, we consider the following $Q(\mathbf{M})$'s:

- 1) maximally collapsing metric learning (MCML) [45].
- 2) distance metric learning (DML) [62]. For the sake of comparison, we remove the first constraint $\sum_{\mathbf{f}_i, \mathbf{f}_j \in \mathcal{S}} \Delta \mathbf{f}_{ij}^\top \mathbf{M} \Delta \mathbf{f}_{ij} \leq c, c > 0$ (\mathcal{S} denotes the set of sample pairs that have the same labels) since (1) this constraint only results in \mathbf{M} being replaced by a scaled version $c^2 \mathbf{M}$, and (2) solving this constraint problem (solving a sparse system of linear equations) may result in \mathbf{M} not being positive definite. See [62] for details.
- 3) least squared-residual metric learning (LSML) [63]. We set the distance weights to be all 1's and no prior metric matrix is given.
- 4) large margin nearest neighbor (LMNN) [20]. Note that the objective function is piecewise linear.

- 5) graph smoothness (GLR). Specifically, the objective function $Q(\mathbf{M})$ we consider here is the *graph Laplacian Regularizer* (GLR) [52], [64]:

$$\sum_{i=1}^N \sum_{j=1}^N \exp \{-(\mathbf{f}_i - \mathbf{f}_j)^\top \mathbf{M} (\mathbf{f}_i - \mathbf{f}_j)\} (z_i - z_j)^2. \quad (39)$$

A small GLR means that signal \mathbf{z} at connected node pairs (z_i, z_j) are similar for a large edge weight $w_{i,j}$, i.e., \mathbf{z} is *smooth* with respect to the variation operator $\mathbf{L}(\mathbf{M})$. GLR has been used in the GSP literature to solve a range of inverse problems, including image denoising [64], deblurring [65], dequantization and contrast enhancement [66], and soft decoding of JPEG [67].

See Table. 1 for the above objective functions, their first derivatives w.r.t. M_{mn} , and their second derivatives w.r.t. γ .

We evaluate PD-cone, HBNB, and SGML on the 14 datasets used in [68], *Sonar* with 208 samples, 60 features, *Madelon* with 2600 samples, 500 features, and *Colon-cancer* with 62 samples, 2000 features, all of which are binary datasets and publicly available in UCI² and LibSVM³. For each of the three above optimization schemes, we randomly split (with random seed 0) a dataset into $P = \text{round}(N/4)$ folds, run optimization on each fold and take the average of the converged objective values. We run the similar experiments on datasets *Madelon* and *Colon-cancer*, except that we only run the first 10 of P folds of the data and take the average. We apply the same data normalization scheme in [68] that 1) subtracts the mean and divides by the standard deviation feature-wise, and 2) normalizes to unit length sample-wise. We add 10^{-12} noise (random seed 0) to the dataset to avoid NaN's due to data normalization on small number of samples.

The experimental settings of PD-cone, HBNB and SGML are listed in Table 2. The converged objective values are reported in Tables 3 and 4. Both tables show that, given PD-cone being a ground-truth scheme, SGML consistently achieves larger objective values than HBNB in DML convex maximization problem, generally achieves smaller objective values than HBNB in MCML, LSML and GLR convex minimization problems, except for LMNN minimization problem whose objective is piecewise linear and not differentiable everywhere.

All three optimization schemes are implemented in Matlab. Figs. 4 and 5 show the total running time, as well as most time-consuming components of PD-cone, HBNB, and SGML, on datasets *Madelon* and *Colon-cancer*. Both figures show that eigen-decomposition for PD-cone and computation of the smallest eigenvalue for HBNB on large matrices entail high computation complexity. In contrast, the time complexity of SGML is significantly lower than PD-cone and HBNB for datasets with high-

2. <https://archive.ics.uci.edu/ml/datasets.php>

3. <https://www.csie.ntu.edu.tw/~cjlin/libsvmtools/datasets/binary.html>

dimensional features, where our computation time includes the total time of computing the first eigenvector using LOBPCG with warm start, solving linear programs using Matlab `linprog` (used in Steps 3-8 in Algorithm 1) and Gurobi Matlab interface LP solver⁴ (used in Steps 12-17 in Algorithm 1) and Frank-Wolfe step size optimization.

6.2 Binary classification

Further, we evaluate the performance of SGML on binary classification using the same 14 binary datasets used in [68]. Since tailoring a metric learning algorithm to a classifier is out of the scope of this paper, we heuristically adopt our learned M in the following three classifiers:

- 1) K-nearest neighbor implemented by authors of Information-Theoretic Metric Learning⁵ (ITML). We set $K = 3$.
- 2) Mahalanobis⁶. The predicted class of sample x is the one that yields a smaller Mahalanobis distance: $\sqrt{(x - \mu_i)^\top M(x - \mu_i)}$, $i \in \{1, -1\}$, where μ_i denotes the mean value of each feature in one class of the training data.
- 3) A graph-based classifier. Specifically, we first find an optimal M via (39) (SGML) given label vector z with 100% known (fixed) labels. Then we re-define z so that z consists of the same known (fixed) labels and the unknown labels. Next, we find an optimal z , again, via (39) (a quadratic program solved by CVX, and then take the sign of the solution as the predicted labels), with M fixed.

As done in [68], we randomly (with random seeds 0-9) split each dataset into 60% training and 40% test sets and take the average and standard deviation of accuracy of 10 runs.

We compare SGML against the best 9 out of 13 metric learning algorithms tested in [68], in terms of the average classification accuracy of all 14 tested datasets. Table 5 shows that, with a GLR objective, SGML on three classifiers has competitive performance in 7 out of 14 datasets, which may be due to the fact that GLR promotes the smoothness within each piece of the binary label signal and the difference at the boundary of the two pieces of the label signal.

7 CONCLUSION

A common challenge in metric learning is to efficiently handle the restriction $M \succ 0$ of the solution metric M to the positive definite (PD) cone. Circumventing full eigen-decomposition, we propose a fast, general optimization

4. https://www.gurobi.com/documentation/9.0/examples/linprog_m.html

5. <http://www.cs.utexas.edu/users/pjain/itml/download/itml-1.2.tar.gz>

6. https://github.com/LEMINHDONG161/BSS-Euclidean-Mahalanobis_Bayes_Classifier/blob/master/mahalanobis_classifier.m

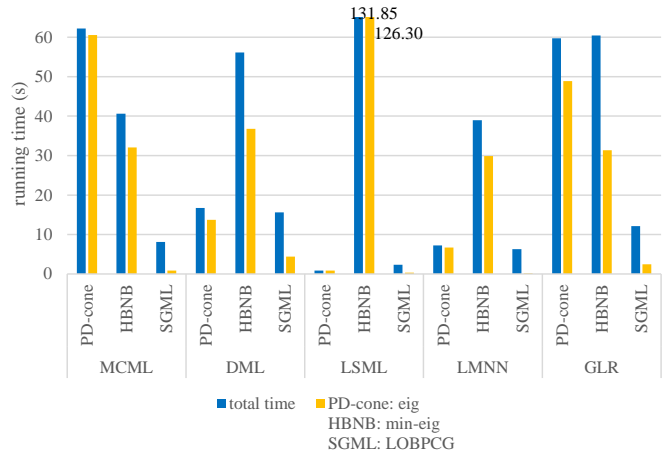


Fig. 4. Running time on *Madelon* of different methods PD-cone, HBNB, and SGML on various objective functions MCML, DML, LSML, LMNN and GLR. Numbers for running time (s) added to the bars exceed y-axis.

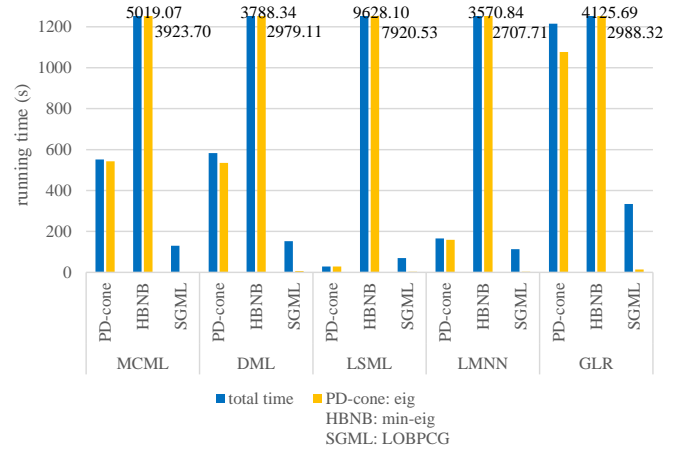


Fig. 5. Running time on *Colon-cancer* of different methods PD-cone, HBNB, and SGML on various objective functions MCML, DML, LSML, LMNN and GLR. Numbers for running time (s) added to the bars exceed y-axis.

framework capable of minimizing any convex and differentiable objective $Q(M)$. The key theoretical foundation is Gershgorin disc alignment (GDA), where we prove that the Gershgorin disc left-ends of a generalized graph Laplacian matrix corresponding to a balanced, irreducible signed graph can be perfectly aligned via a similarity transform. This enables us to write tightest possible signal-adaptive linear constraints to replace the PD cone constraint, allowing us to solve the optimization as linear programs via the Frank-Wolfe method. We envision that GDA can also be applied to other convex optimization problems with PD cone constraints, such as semi-definite programs (SDP).

REFERENCES

- [1] D. Alfke and M. Stoll, “Semi-supervised classification on non-sparse graphs using low-rank graph convolutional networks,” *CoRR*, vol. abs/1905.10224, 2019.

TABLE 1
Tested convex and (partially) differentiable objective functions $Q(\mathbf{M})$'s. $d_{\mathbf{M}}(i, j) = \Delta \mathbf{f}_{ij}^\top \mathbf{M} \Delta \mathbf{f}_{ij}$.

	MCML	DML	LSML	LMNN	GLR
$Q(\mathbf{M})$	$\sum_{i,j: y_j = y_i} d_{\mathbf{M}}(i, j) + \sum_i \log \sum_{k \neq i} \exp \{-d_{\mathbf{M}}(i, k)\}$	$\sum_{\mathbf{f}_i, \mathbf{f}_j \in \mathcal{D}} \sqrt{d_{\mathbf{M}}(i, j)}$	$\sqrt{d_{\mathbf{M}}(a, b)} > \sqrt{d_{\mathbf{M}}(c, d)} \cdot \sum_{\mathbf{f}_a, \mathbf{f}_b \in \mathcal{S}, \mathbf{f}_c, \mathbf{f}_d \in \mathcal{D}} \left(\frac{\sqrt{d_{\mathbf{M}}(a, b)}}{\sqrt{d_{\mathbf{M}}(c, d)}} - \sqrt{d_{\mathbf{M}}(c, d)} \right)^2$	$(1 - \mu) \sum_{i, j \sim i} d_{\mathbf{M}}(i, j) + \mu \sum_{i, j \sim i} \sum_l (1 - y_{il}) \left[1 + d_{\mathbf{M}}(i, j) - d_{\mathbf{M}}(i, l) \right]_+$	$\sum \exp \{-d_{\mathbf{M}}(i, j)\} (z_i - z_j)^2$

TABLE 2
Experimental settings of compared optimization schemes.

Parameters	PD-cone	HBNB	SGML
main tol		1.00E-05	
max main iter.		1.00E+03	
GD step size	$t_0 = 0.1/N$ $t_k = 1.01t_{k-1}$, if GD yields better obj. $t_k = t_{k-1}/2$, o.w.[20]	-	-
dia/offdia tol	-	1.00E-03	
max dia/offdia/FW iter.		1.00E+03	
LP optimality tol		1.00E-02	
LP interior-point tol	-	1.00E-04	
FW step size		NR/GD 0.5 tol	

[2] P. C. Mahalanobis, "On the generalized distance in statistics," *Proceedings of the National Institute of Sciences of India*, vol. 2, no. 1, pp. 49–55, April 1936.

[3] M. Vetterli, J. Kovacevic, and V. Goyal, *Foundations of Signal Processing*. Cambridge University Press, 2014.

[4] Y. Mu, "Fixed-rank supervised metric learning on Riemannian manifold," in *AAAI*, Feb. 2016, pp. 1941–1947.

[5] J. Zhang and L. Zhang, "Efficient stochastic optimization for low-rank distance metric learning," in *AAAI*, Feb. 2017, pp. 933–939.

[6] K. Song, F. Nie, J. Han, and X. Li, "Parameter free large margin nearest neighbor for distance metric learning," in *Thirty-First AAAI Conference on Artificial Intelligence*, 2017.

[7] L. Luo and H. Huang, "Matrix variate gaussian mixture distribution steered robust metric learning," in *Thirty-Second AAAI Conference on Artificial Intelligence*, 2018.

[8] L. Luo, J. Xu, C. Deng, and H. Huang, "Robust metric learning on grassmann manifolds with generalization guarantees," in *Proceedings of the AAAI Conference on Artificial Intelligence*, vol. 33, 2019, pp. 4480–4487.

[9] S. Chen, C. Gong, J. Yang, Y. Tai, L. Hui, and J. Li, "Data-adaptive metric learning with scale alignment," in *Proceedings of the AAAI Conference on Artificial Intelligence*, vol. 33, 2019, pp. 3347–3354.

[10] N. Parikh and S. Boyd, "Proximal algorithms," *Foundations and Trends in Optimization*, vol. 1, no. 3, pp. 127–239, Jan. 2014.

[11] G.-J. Qi, J. Tang, Z.-J. Zha, T.-S. Chua, and H.-J. Zhang, "An efficient sparse metric learning in high-dimensional space via l_1 -penalized log-determinant regularization," in *ICML*, June 2009, pp. 841–848.

[12] D. Lim, G. Lanckriet, and B. McFee, "Robust structural metric learning," in *ICML*, June 2013, pp. 615–623.

[13] W. Liu, C. Mu, R. Ji, S. Ma, J. R. Smith, and S.-F. Chang, "Low-rank similarity metric learning in high dimensions," in *AAAI*, Jan. 2015, p. 27922799.

[14] C. Yang, G. Cheung, and V. Stankovic, "Alternating binary classifier and graph learning from partial labels," in *APSIPA*, Nov. 2018, pp. 1137–1140.

[15] T. Biyikoglu, J. Leydold, and P. F. Stadler, "Nodal domain theorems and bipartite subgraphs," *The Electronic Journal of Linear Algebra*, vol. 13, pp. 344–351, Jan. 2005.

[16] R. S. Varga, *Gershgorin and his circles*. Springer, 2004.

[17] C. Papadimitriou and K. Steiglitz, *Combinatorial Optimization*. Dover Publications, Inc, 1998.

[18] M. Jaggi, "Revisiting Frank-Wolfe: Projection-free sparse convex optimization," in *ICML*, Jun. 2013, pp. 427–435.

[19] A. V. Knyazev, "Toward the optimal preconditioned eigen-solver: Locally optimal block preconditioned conjugate gradient method," *SIAM Journal on Scientific Computing*, vol. 23, no. 2, pp. 517–541, 2001.

[20] K. Q. Weinberger and L. K. Saul, "Distance metric learning for large margin nearest neighbor classification," *Journal of Machine Learning Research*, vol. 10, no. 2, pp. 207–244, Feb. 2009.

[21] G. Tsagkatakis and A. Savakis, "Manifold modeling with learned distance in random projection space for face recognition," in *2010 20th International Conference on Pattern Recognition*. IEEE, 2010, pp. 653–656.

[22] M. Schultz and T. Joachims, "Learning a distance metric from relative comparisons," in *Advances in neural information processing systems*, 2004, pp. 41–48.

[23] L. Torresani and K.-c. Lee, "Large margin component analysis," in *Advances in neural information processing systems*, 2007, pp. 1385–1392.

[24] S. Mika, G. Ratsch, J. Weston, B. Scholkopf, and K.-R. Mullers, "Fisher discriminant analysis with kernels," in *Neural networks for signal processing IX: Proceedings of the 1999 IEEE signal processing society workshop (cat. no. 98th8468)*. Ieee, 1999, pp. 41–48.

[25] F. Wang and C. Zhang, "Feature extraction by maximizing the average neighborhood margin," in *2007 IEEE Conference on Computer Vision and Pattern Recognition*. IEEE, 2007, pp. 1–8.

[26] B. Nguyen, C. Morell, and B. De Baets, "Supervised distance metric learning through maximization of the jeffrey divergence," *Pattern Recognition*, vol. 64, pp. 215–225, 2017.

[27] J. Lu, J. Hu, and J. Zhou, "Deep metric learning for visual understanding: An overview of recent advances," *IEEE Signal Processing Magazine*, vol. 34, no. 6, pp. 76–84, 2017.

[28] R. Hadsell, S. Chopra, and Y. LeCun, "Dimensionality reduction by learning an invariant mapping," in *2006 IEEE Computer Society Conference on Computer Vision and Pattern Recognition (CVPR'06)*, vol. 2. IEEE, 2006, pp. 1735–1742.

[29] X. Cai, C. Wang, B. Xiao, X. Chen, and J. Zhou, "Deep nonlinear metric learning with independent subspace analysis for face verification," in *Proceedings of the 20th ACM international conference on Multimedia*, 2012, pp. 749–752.

[30] Y. Taigman, M. Yang, M. Ranzato, and L. Wolf, "Deepface: Closing the gap to human-level performance in face verification," in *Proceedings of the IEEE conference on computer vision and pattern recognition*, 2014, pp. 1701–1708.

[31] J. Hu, J. Lu, and Y.-P. Tan, "Discriminative deep metric learning for face verification in the wild," in *Proceedings of the IEEE conference on computer vision and pattern recognition*, 2014, pp. 1875–1882.

[32] Y. Sun, Y. Chen, X. Wang, and X. Tang, "Deep learning face representation by joint identification-verification," in *Advances in neural information processing systems*, 2014, pp. 1988–1996.

[33] J. Lu, G. Wang, W. Deng, P. Moulin, and J. Zhou, "Multi-manifold deep metric learning for image set classification," in *Proceedings of the IEEE conference on computer vision and pattern recognition*, 2015, pp. 1137–1145.

[34] J. Hu, J. Lu, and Y.-P. Tan, "Deep transfer metric learning," in *Proceedings of the IEEE conference on computer vision and pattern recognition*, 2015, pp. 325–333.

[35] J. Wang, Y. Song, T. Leung, C. Rosenberg, J. Wang, J. Philbin, B. Chen, and Y. Wu, "Learning fine-grained image similarity with deep ranking," in *Proceedings of the IEEE Conference on Computer Vision and Pattern Recognition*, 2014, pp. 1386–1393.

[36] E. Hoffer and N. Ailon, "Deep metric learning using triplet network," in *International Workshop on Similarity-Based Pattern Recognition*. Springer, 2015, pp. 84–92.

[37] F. Schroff, D. Kalenichenko, and J. Philbin, "Facenet: A unified embedding for face recognition and clustering," in *Proceedings of*

TABLE 3

Converged objective values. The better objective values between HBNB and SGML are in bold. (avg of $P = \text{round}(N/4)$ runs (run 4 samples at a time); split data into K folds and run K times; timed datasets (on *madelon* and *colon-cancer*) run the first 10 folds and then take the avg.; M initialized as diagonal entries equal to 1 and first off-diagonal entries equal to 0.1; tolerance 1e-5; random seed 0; Intel Core i7-9700K 3.60GHz Windows 10 64bit 32GB of RAM)

$Q(M)$	Dataset (N, K)	Australian (690,14)	Breastcancer (683,10)	Diabetes (768,8)	Fourclass (862,2)	German (1000,24)	Haberman (206,3)	Heart (270,13)	ILPD (583,10)
MCML	PD-cone	5.21E-03	1.17E-02	3.46E-02	9.11E-01	1.12E-02	2.86E-01	2.80E-03	3.78E-02
	HBNB	3.49E-01	8.96E-02	5.75E-01	1.07E+00	2.13E-01	4.56E-01	3.56E-01	2.65E-01
	SGML	1.74E-01	4.26E-02	4.27E-01	1.00E+00	9.71E-02	4.14E-01	1.37E-01	2.23E-01
DML	PD-cone	1.62E+01	1.75E+01	1.16E+01	6.63E+00	1.80E+01	6.47E+00	1.57E+01	1.14E+01
	HBNB	8.64E+00	9.18E+00	8.11E+00	6.87E+00	7.20E+00	6.24E+00	8.86E+00	7.37E+00
	SGML	1.01E+01	1.01E+01	8.97E+00	6.95E+00	9.32E+00	6.57E+00	9.99E+00	8.33E+00
LSML	PD-cone	8.56E-03	1.25E-03	5.68E-03	4.73E-01	1.71E-02	7.54E-02	7.57E-03	1.43E-02
	HBNB	2.33E-02	1.03E-03	2.32E-02	5.20E-01	3.27E-02	1.24E-01	1.49E-02	6.10E-02
	SGML	3.54E-02	5.15E-04	7.88E-02	2.48E-02	1.16E-02	7.32E-02	2.21E-02	6.69E-02
LMNN	PD-cone	7.33E+00	6.72E+00	6.55E+00	8.64E+00	6.21E+00	6.49E+00	7.38E+00	6.12E+00
	HBNB	8.94E+00	7.93E+00	9.32E+00	9.44E+00	7.88E+00	8.69E+00	8.94E+00	8.18E+00
	SGML	9.94E+00	8.20E+00	9.57E+00	9.68E+00	8.69E+00	8.40E+00	1.00E+01	9.15E+00
GLR	PD-cone	3.50E-03	1.13E-03	3.79E-02	1.66E+00	1.04E-03	6.29E-01	1.34E-03	2.58E-02
	HBNB	1.56E-01	5.29E-02	2.27E-01	1.57E+00	1.27E-01	6.69E-01	1.43E-01	1.94E-01
	SGML	1.25E-01	2.55E-02	2.79E-01	1.61E+00	5.92E-02	6.96E-01	1.11E-01	1.48E-01

TABLE 4

Continuation of Table 3 on other datasets. The better objective values between HBNB and SGML are in bold. All problems minimize $Q(M)$'s except DML.

$Q(M)$	dataset (N, K)	Liverdisorders (345,6)	Monk1 (556,6)	Pima (768,8)	Planning (182,12)	Voting (435,16)	WDBC (569,30)	Sonar (208,60)	madelon (2600,500)	colon-cancer (62,2000)
MCML	PD-cone	1.85E-01	1.12E-01	3.95E-02	3.52E-02	1.01E-02	9.34E-03	2.14E-03	9.95E-04	6.01E-03
	HBNB	8.59E-01	1.14E+00	5.46E-01	2.91E-01	1.06E-01	1.53E-01	4.24E-01	4.48E-01	1.64E-01
	SGML	6.55E-01	7.28E-01	4.35E-01	1.73E-01	2.04E-02	5.40E-02	1.23E-01	1.64E-02	3.83E-02
DML	PD-cone	9.64E+00	1.04E+01	1.15E+01	1.24E+01	1.94E+01	2.68E+01	3.17E+01	8.92E+01	1.56E+02
	HBNB	8.03E+00	8.26E+00	8.01E+00	7.29E+00	9.08E+00	7.74E+00	6.75E+00	6.74E+00	5.21E+00
	SGML	8.56E+00	8.96E+00	8.79E+00	8.10E+00	1.05E+01	1.04E+01	1.08E+01	1.12E+01	9.28E+00
LSML	PD-cone	8.80E-03	3.23E-03	4.33E-03	5.07E-03	3.10E-03	2.09E-03	6.86E-03	2.34E-03	1.20E-02
	HBNB	6.21E-02	2.89E-02	2.64E-02	1.88E-02	9.41E-03	9.63E-03	1.79E-02	6.60E-03	1.25E-02
	SGML	1.32E-01	9.05E-02	7.48E-02	4.39E-02	9.76E-03	3.61E-03	4.72E-03	3.99E-06	2.96E-04
LMNN	PD-cone	6.89E+00	8.09E+00	6.59E+00	6.06E+00	6.97E+00	6.92E+00	8.20E+00	7.98E+00	6.50E+00
	HBNB	9.43E+00	1.03E+01	9.21E+00	8.19E+00	8.20E+00	8.35E+00	9.83E+00	1.04E+01	8.59E+00
	SGML	9.85E+00	1.05E+01	9.60E+00	8.58E+00	9.50E+00	9.53E+00	1.23E+01	1.11E+01	8.49E+00
GLR	PD-cone	2.15E-01	1.19E-01	4.08E-02	1.90E-03	1.15E-03	1.00E-03	1.00E-03	9.88E-04	9.75E-04
	HBNB	4.16E-01	3.67E-01	2.54E-01	1.45E-01	8.88E-02	1.53E-01	7.78E-01	8.88E-01	7.23E-01
	SGML	4.32E-01	5.04E-01	2.73E-01	1.21E-01	2.69E-02	3.65E-02	8.47E-02	8.80E-02	6.02E-02

TABLE 5

Classification accuracy of metric learning algorithms. avg. of 10 runs (random seeds 0-9). Results of competing schemes are copied from [68].

Datasets	RVML	PLML	mmLMNN	GMML	DMLMJ	SCML	DMLE	R2LML	LMLIR	SGML (prop.)
	[69]	[70]	[20]	[47]	[71]	[72]	[46]	[73]	[68]	3-NN Mahalanobis Graph
australian	83.0±1.6	80.5±1.1	82.5±2.6	84.4±1.0	83.9±1.3	82.3±1.4	82.6±1.5	84.7±1.3	85.1±1.9	83.3±1.2 84.8±1.3 85.3±1.7
breastcancer	95.8±1.1	96.4±0.9	96.7±1.0	97.3±0.8	96.6±0.8	97.0±0.9	97.0±1.1	97.0±0.7	96.4±2.1	97.6±1.0 98.0±0.6 97.6±0.7
diabetes	71.0±2.6	68.5±2.0	72.2±1.9	74.2±2.6	71.5±3.1	71.5±2.2	72.6±2.0	73.8±1.4	75.9±1.9	71.6±1.8 70.5±2.5 70.3±1.4
fourclass	70.5±1.4	72.4±2.4	75.6±1.4	76.1±1.9	76.1±1.9	75.5±1.4	75.6±1.4	76.1±1.9	79.9±0.9	74.5±2.4 71.1±1.6 78.0±1.2
german	71.7±1.8	70.0±2.9	68.9±1.8	71.6±1.1	69.3±2.7	70.9±2.7	72.0±2.1	72.9±1.8	73.7±1.6	71.6±1.7 70.9±1.3 70.0±0.0
haberman	66.7±2.3	67.1±3.1	69.0±2.7	71.2±3.4	68.5±3.2	69.2±2.5	70.8±3.5	71.1±3.4	74.4±3.7	68.8±3.9 66.6±6.3 73.6±0.3
heart	77.7±4.1	75.1±3.2	79.4±3.7	81.2±2.7	80.6±2.8	79.0±3.2	77.9±3.1	82.0±3.8	83.1±3.2	81.0±3.4 83.2±3.6 83.6±3.5
ILPD	68.0±2.9	67.4±3.0	66.8±2.1	67.1±2.2	68.0±1.6	68.0±2.9	68.8±2.7	65.9±2.2	69.6±2.7	65.2±2.4 59.1±2.4 71.3±0.2
liverdisorders	64.6±3.9	62.2±2.5	62.0±3.5	63.8±5.4	60.9±3.8	61.7±4.6	61.8±2.7	66.8±3.7	66.7±3.6	69.5±3.3 68.8±5.9 72.1±3.0
monk1	89.2±2.7	96.6±2.7	90.3±2.6	75.0±2.6	87.7±3.8	97.5±0.9	99.9±0.3	89.2±1.5	95.0±7.2	84.6±5.1 66.3±3.0 71.1±3.7
pima	69.5±1.7	68.4±2.2	72.5±2.7	73.0±1.8	71.1±2.8	71.1±2.6	72.1±2.4	72.3±1.5	74.6±2.0	73.4±1.3 73.6±2.0 69.2±1.5
planning	55.1±7.4	60.8±5.5	54.7±0.9	65.2±5.5	64.3±2.9	61.9±5.0	60.1±5.5	63.9±3.4	67.5±6.5	62.8±4.1 48.8±4.8 71.3±0.7
voting	95.8±1.3	95.5±1.0	95.4±0.9	95.2±1.9	95.3±1.1	95.0±1.3	93.1±1.9	96.3±1.2	93.2±3.9	96.4±1.4 94.3±2.0 94.8±1.6
WDBC	96.6±1.3	96.4±0.9	97.4±1.0	96.7±0.8	97.3±1.9	97.0±0.9	96.7±0.5	96.9±1.7	96.6±1.0	96.6±0.9 94.8±1.2 96.2±1.1
average	76.7	76.9	77.3	77.9	77.9	78.4	78.6	79.2	80.8	78.4 75.1 5
# of best	0	0	1	0	0	0	1	0	5	1 1 5

the IEEE conference on computer vision and pattern recognition, 2015, pp. 815–823.

[38] S. Bell and K. Bala, “Learning visual similarity for product design with convolutional neural networks,” *ACM transactions on graphics (TOG)*, vol. 34, no. 4, pp. 1–10, 2015.

[39] H. Oh Song, Y. Xiang, S. Jegelka, and S. Savarese, “Deep metric learning via lifted structured feature embedding,” in *Proceedings of the IEEE conference on computer vision and pattern recognition*, 2016, pp. 4004–4012.

[40] Y. Cui, F. Zhou, Y. Lin, and S. Belongie, “Fine-grained categorization and dataset bootstrapping using deep metric learning with humans in the loop,” in *Proceedings of the IEEE conference on computer vision and pattern recognition*, 2016, pp. 1153–1162.

[41] H. Shi, Y. Yang, X. Zhu, S. Liao, Z. Lei, W. Zheng, and S. Z. Li, “Embedding deep metric for person re-identification: A study against large variations,” in *European conference on computer vision*. Springer, 2016, pp. 732–748.

[42] I. Lim, A. Gehre, and L. Kobbelt, “Identifying style of 3d shapes using deep metric learning,” in *Computer Graphics Forum*, vol. 35, no. 5. Wiley Online Library, 2016, pp. 207–215.

[43] O. Batchelor and R. Green, “Object recognition by stochastic metric learning,” in *Asia-Pacific Conference on Simulated Evolution and Learning*. Springer, 2014, pp. 798–809.

[44] K. Sohn, “Improved deep metric learning with multi-class n-pair loss objective,” in *Advances in neural information processing systems*, 2016, pp. 1857–1865.

[45] A. Globerson and S. T. Roweis, “Metric learning by collapsing classes,” in *Advances in neural information processing systems*, 2006, pp. 451–458.

[46] Y. Ying and P. Li, “Distance metric learning with eigenvalue optimization,” *Journal of machine Learning research*, vol. 13, no. Jan, pp. 1–26, 2012.

[47] P. Zadeh, R. Hosseini, and S. Sra, “Geometric mean metric learning,” in *ICML*, June 2016, pp. 2464–2471.

[48] Y. Bai, G. Cheung, F. Wang, X. Liu, and W. Gao, “Reconstruction-cognizant graph sampling using Gershgorin disc alignment,” in *ICASSP*, May 2019, pp. 5396–5400.

[49] Y. Bai, F. Wang, G. Cheung, Y. Nakatsukasa, and W. Gao, “Fast graph sampling set selection using Gershgorin disc alignment,” *IEEE Transactions on Signal Processing*, March 2020.

[50] C. Yang, G. Cheung, and W. Hu, “Fast graph metric learning via Gershgorin disc alignment,” in *IEEE International Conference on Acoustics, Speech and Signal Processing*, May 2020.

[51] A. Ortega, P. Frossard, J. Kovaevi, J. M. F. Moura, and P. Vandergheynst, “Graph signal processing: Overview, challenges, and applications,” *Proceedings of the IEEE*, vol. 106, no. 5, pp. 808–828, May 2018.

[52] D. I. Shuman, S. K. Narang, P. Frossard, A. Ortega, and P. Vandergheynst, “The emerging field of signal processing on graphs: Extending high-dimensional data analysis to networks and other irregular domains,” *IEEE Signal Processing Magazine*, vol. 30, pp. 83–98, May 2013.

[53] M. Milgram, “Irreducible graphs,” *Journal Of Combinatorial Theory (B)*, vol. 12, pp. 6–31, Feb. 1972.

[54] G. Cheung, E. Magli, Y. Tanaka, and M. K. Ng, “Graph spectral image processing,” *Proceedings of the IEEE*, vol. 106, no. 5, pp. 907–930, May 2018.

[55] G. H. Golub and C. F. Van Loan, *Matrix Computations*, 3rd ed. The Johns Hopkins University Press, 1996.

[56] R. Horn and C. Johnson, *Matrix Analysis*. Cambridge University Press, 2012.

[57] D. Cartwright and F. Harary, “Structural balance: a generalization of heider’s theory,” *Psychological Review*, vol. 63, no. 5, pp. 277–293, 1956.

[58] J. Leskovec, D. Huttenlocher, and J. Kleinberg, “Signed networks in social media,” in *SIGCHI Conference on Human Factors in Computing Systems*, April 2010, p. 13611370.

[59] S. Boyd and L. Vandenberghe, *Convex Optimization*. Cambridge University Press, 2009.

[60] J. Raphson, *Analysis aequationum universalis*, London, 1690.

[61] W. Hu, X. Gao, G. Cheung, and Z. Guo, “Feature graph learning for 3D point cloud denoising,” *IEEE Transactions on Signal Processing*, vol. 68, pp. 2841–2856, 2020.

[62] E. P. Xing, M. I. Jordan, S. J. Russell, and A. Y. Ng, “Distance metric learning with application to clustering with side-information,” in *Advances in Neural Information Processing Systems 15*, S. Becker, S. Thrun, and K. Obermayer, Eds., Dec. 2003, pp. 521–528.

[63] E. Y. Liu, Z. Guo, X. Zhang, V. Jovic, and W. Wang, “Metric learning from relative comparisons by minimizing squared residual,” in *IEEE International Conference on Data Mining*, Dec. 2012, pp. 978–983.

[64] J. Pang and G. Cheung, “Graph Laplacian regularization for image denoising: Analysis in the continuous domain,” *IEEE Transactions on Image Processing*, vol. 26, no. 4, pp. 1770–1785, April 2017.

[65] Y. Bai, G. Cheung, X. Liu, and W. Gao, “Graph-based blind image deblurring from a single photograph,” *IEEE Transactions on Image Processing*, vol. 28, no. 3, pp. 1404–1418, March 2019.

[66] X. Liu, G. Cheung, X. Ji, D. Zhao, and W. Gao, “Graph-based joint dequantization and contrast enhancement of poorly lit JPEG images,” *IEEE Transactions on Image Processing*, vol. 28, no. 3, pp. 1205–1219, March 2019.

[67] X. Liu, G. Cheung, X. Wu, and D. Zhao, “Random walk graph Laplacian-based smoothness prior for soft decoding of JPEG images,” *IEEE Transactions on Image Processing*, vol. 26, no. 2, pp. 509–524, Feb. 2017.

[68] M. Dong, Y. Wang, X. Yang, and J. Xue, “Learning local metrics and influential regions for classification,” *IEEE Transactions on Pattern Analysis and Machine Intelligence*, vol. 42, no. 6, pp. 1522–1529, June 2020.

[69] M. Perrot and A. Habrard, “Regressive virtual metric learning,” in *Advances in Neural Information Processing Systems 28*, Dec. 2015, pp. 1810–1818.

[70] J. Wang, A. Kalousis, and A. Woznica, “Parametric local metric learning for nearest neighbor classification,” in *Advances in Neural Information Processing Systems 25*, Dec. 2012, pp. 1601–1609.

[71] B. Nguyen, C. Morell, and B. D. Baets, “Supervised distance metric learning through maximization of the jeffrey divergence,” *Pattern Recognition*, vol. 64, pp. 215 – 225, April 2017.

[72] Y. Shi, A. Bellet, and F. Sha, “Sparse compositional metric learning,” in *AAAI Conference on Artificial Intelligence*, July 2014, p. 20782084.

[73] Y. Huang, C. Li, M. Georgopoulos, and G. C. Anagnostopoulos, “Reduced-rank local distance metric learning,” in *Machine Learning and Knowledge Discovery in Databases*, Sept. 2013, pp. 224–239.